

引用格式: SHEN Licui, HUANG Sujuan, CHEN Wei, et al. Inter-core Differential Group Delay Measurement of Seven Core Fiber Based on Spatial Interference Imaging[J]. Acta Photonica Sinica, 2023, 52(7):0706002

沈立翠, 黄素娟, 陈伟, 等. 基于空间干涉成像的七芯光纤芯间群延时差测量[J]. 光子学报, 2023, 52(7):0706002

基于空间干涉成像的七芯光纤芯间群延时差测量

沈立翠, 黄素娟, 陈伟, 闫成, 赵欣鹏

(上海大学 通信与信息工程学院, 特种光纤与光接入网重点实验室, 上海 200444)

摘要:提出了基于空间干涉成像的多芯光纤芯间群延时差的测量方法。用 CCD 记录不同波长下的空间干涉图, 利用干涉图中所有像素点的干涉信息构建三维空间干涉光谱, 并通过光谱分析可得芯间群延时差。搭建了基于空间干涉成像的多芯光纤芯间群延时差测量实验装置, 测量了沟槽辅助型弱耦合七芯光纤芯间群延时差。该方法的测量装置简单, 测量精度可达 10^{-4} ps/m, 不仅可测量两芯间的延时差还可同时测量任意相邻的多个芯的芯间延时差。测量时使用三维调节台加 CCD 的组合使得待测纤芯的选择激发更加简单。此外, 还研究了多芯光纤芯间延时差的弯曲依赖性, 结果显示, 随着弯曲半径的增大, 多芯光纤芯间群延时差不断减小。

关键词:空间干涉成像; 光谱分析; 弱耦合七芯光纤; 芯间群延时差; 弯曲依赖性

中图分类号: TN253

文献标识码: A

doi: 10.3788/gzxb20235207.0706002

0 引言

使用多芯光纤(Multicore Fiber, MCF)的不同纤芯作为独立并行的空间通道来传输不同信息, 可解决传统单模光纤(Single Mode Fiber, SMF)的传输容量限制问题。近年来, MCF 已经成为空分复用(Space-Division Multiplexing, SDM)系统^[1-5]和微波光子学(Microwave Photonics, MWP)领域^[6-10]的重点研究对象。MCF 的芯间群延时差(Differential Group Delay, DGD)是一个关键的物理参数。在 SDM 系统中 MCF 的传播延时差太大会降低可实现的符号速率、传输距离, 并增加接收器的设计和信号处理的复杂度^[11, 12]。在 MWP 信号处理中, 为了使 MCF 作为可调谐采样(True-Time Delay Line, TTDL)工作, 每个纤芯需要不同的群延时和色散特性, 以实现光波长的可调谐性^[13]。

目前 MCF 的芯间群延时差的测量方法主要有: 脉冲响应法、白光光谱干涉法、差分相移法以及光谱干涉法。2014 年, 日本的 SAKAMOTO T 等^[14]使用脉冲响应法测量了四芯光纤的芯间群延时差, 该方法测量精度较低, 对脉冲信号质量要求高, 且所需测量光纤长度较长, 一般为几公里到几十公里。白光光谱干涉法是基于马赫-曾德尔干涉仪原理的测量方法。2015 年, LEE H J 等^[15]使用两个空间光调制器将 SMF 的基模与 MCF 多个芯的模式任意相干叠加, 以构成马赫-曾德尔型多径干涉仪, 通过测量输出光谱的干涉条纹周期可推算出不同芯间折射率差, 它可测量长度较短的 MCF(1 m), 但其实验装置复杂, 对光路调节的精度要求很高。2020 年, SASAKI Y 等^[16]使用差分相移法测量了四芯光纤的芯间群延时差, 该方法可直接通过相位差获得任意两芯之间的延时差, 但它需要对信号进行滤波、放大以及采样处理, 测量成本较高, 且数据处理复杂。2019 年, GARCIA S 等^[17]使用光谱干涉法测量研究了弯曲对七芯光纤芯间群延时差的影响, 该方法使用多芯光纤本身作为干涉仪, 不需要搭建复杂的干涉仪, 具有较好的抗干扰和环境变化的能力, 但它对

基金项目:国家自然科学基金(Nos. 62075125, 62275148), 上海市科委项目(Nos. 19DZ2294000, 20DZ2204900), 江苏省产业前瞻与关键核心技术-重点项目(No. BE20222055-4)

第一作者:沈立翠, slicui@163.com

通讯作者:黄素娟, sjhuang@shu.edu.cn

收稿日期:2022-10-17; **录用日期:**2023-03-15

<http://www.photon.ac.cn>

光谱仪的分辨率要求较高,且测量时需要使用光纤扇入扇出模块来实现单模光纤与多芯光纤之间的光源耦合,由于该模块本身就存在延时,会导致测量结果出现误差。

本文提出了基于空间干涉成像的多芯光纤芯间群延时差测量方法。多芯光纤中不同芯间的结构差异和弯曲都会引起不同芯的群延时存在差异,导致不同芯在激光下在空间上发生干涉。使用CCD记录不同波长下的空间干涉图像,并从干涉图像中提取空间所有点的干涉光谱,通过光谱分析可获得多芯光纤芯间群延时差。

1 测量原理

对于沟槽辅助型弱耦合多芯光纤,其芯间距较大可忽略芯间耦合^[18]。假设每个芯独立,则其任意一个芯 m (m 为纤芯的编号) 中的导波模传输常数 β_m 可表示为

$$\beta_m = k_0 n_{\text{eff},m} = \sqrt{k_0^2 n_m^2 - \frac{U^2}{a_m^2}} \quad (1)$$

式中, k_0 为真空中的波数, $n_{\text{eff},m}$ 为芯 m 中导波模的有效折射率, n_m 为芯 m 的折射率, a_m 为芯 m 的半径, U 为阶跃折射率光纤的归一化横向相位参数,可通过求解光纤模式特征方程获得。将传播常数对角频率求导可得长度为 L 的多芯光纤中任意芯的群延时为^[19]

$$\tau_m = \frac{d\beta_m}{d\omega} L = \frac{L}{c\beta_m} \left(k_0^2 n_m^2 - 2\pi n_m \frac{dn_m}{d\lambda} + \frac{2\pi}{a_m^2 k_0^2} \frac{dU}{d\lambda} \right) \quad (2)$$

在七芯光纤中当激光只耦合到中间纤芯与外围两个相邻的纤芯中时,由于不同芯具有不同群延时,在任意空间点 (x, y) 处三个芯会两两相干叠加发生干涉。令中间纤芯的编号为 0, 当使用系数 $A_n(x, y)$ ($n=1, 2, \dots, 6$) 将中间芯与外围任意芯 n 的电场关联时可得^[20]

$$E_n(x, y, \omega) = A_n(x, y) E_0(x, y, \omega) \exp(i\omega\Delta\tau_n) \quad (3)$$

式中, E_0 和 E_n 分别为中间芯和外围任意芯 n 的电场分布, $\Delta\tau_n$ 是中间芯与外围任意芯 n 的芯间群延时差。中间芯与两个相邻的外围芯 p 和芯 q 相干叠加的总电场分布可表示为

$$E_{\text{total}} = E_0(x, y, \omega) [1 + A_p(x, y) \exp(i\omega\Delta\tau_p) + A_q(x, y) \exp(i\omega\Delta\tau_q)] \quad (4)$$

则其总干涉光强可表示为

$$I_{\text{total}} = E_{\text{total}} \cdot E_{\text{total}}^* = I_0(x, y, \omega) \{1 + A_p^2 + A_q^2 + 2A_p \cos(\omega\Delta\tau_p) + 2A_q \cos(\omega\Delta\tau_q) + 2A_p A_q \cos[\omega(\Delta\tau_p - \Delta\tau_q)]\} \quad (5)$$

式中, $I_0(x, y, \omega)$ 为中间纤芯的导波模的光强分布。从式(5)中可看出,在多芯光纤出射端,空间中任意一点 (x, y) 处的干涉光强值随频率的变化而发生周期性的变化。因此,对式(5)关于角频率 ω 做傅里叶变换可得多芯光纤的芯间群延时差。

$$F(x, y, \tau) = F_0(x, y, \tau) (1 + A_p^2 + A_q^2) + A_p [F_0(x, y, \tau - \Delta\tau_p) + F_0(x, y, \tau + \Delta\tau_p)] + A_q [F_0(x, y, \tau - \Delta\tau_q) + F_0(x, y, \tau + \Delta\tau_q)] + A_p A_q \{ [F_0(x, y, \tau - (\Delta\tau_p - \Delta\tau_q))] + F_0[x, y, \tau + (\Delta\tau_p - \Delta\tau_q)] \} \quad (6)$$

式中, $F_0(x, y, \tau)$ 是 $I_0(x, y, \omega)$ 的傅里叶变换;等式右边第二项为中间芯与外围芯 p 的干涉项,当 $\tau = \pm\Delta\tau_p$ 时会产生一个尖峰,为两个芯中基模的光学拍;第三项为中间芯与外围芯 q 的干涉项,在 $\tau = \pm\Delta\tau_q$ 时有一个尖峰出现;第四项为外围芯 p 和芯 q 的芯间干涉项,在 $\tau = \pm(\Delta\tau_p - \Delta\tau_q)$ 时会出现一个尖峰。所以当同时激发多芯光纤的三个芯时由其干涉光谱经傅里叶变换取模值相加后可得三个包含芯间群延时差的尖峰,而当只激发两个芯,只有一个尖峰出现。

多芯光纤中的芯间群延时差不仅与光纤本身的结构有关,还受到弯曲的影响。相较于未弯曲时的纤芯有效折射率,由弯曲引起的纤芯有效折射率分布可表示为^[21]

$$n_{\text{eff},m} \approx n_{\text{eff},m} \left(1 + \frac{r_m}{R_b} \cos\theta_m \right) \quad (7)$$

式中, $n_{\text{eff},m}$ 为芯 m 弯曲时的有效折射率, R_b 为弯曲半径, (r, θ) 是图 1(a) 中 (x, y) 笛卡尔坐标系对应的极坐标系。从式(7)可看出,当纤芯 m 和多芯光纤中心的连接线与曲率面形成的夹角 $\theta = k\pi$, $k \in Z$ 时,由弯曲引起

的有效折射率变化最大,而当 $\theta = \pi/2 + k\pi, k \in Z$ 时由弯曲引起的折射率变化为零,即弯曲时的有效折射率与未弯曲时的有效折射率相同。当七芯光纤沿 x 轴方向弯曲时,其由弯曲引起的纤芯的折射率变化如图1所示。根据式(7)可知,图1(a)中位于第一和第四象限的纤芯的有效折射率会变大,而位于第二和第三象限的纤芯的有效折射率则会变小。图1(b)展示了纤芯0、2和5在弯曲及未弯曲时的折射率分布对比,图中直线表示的是未弯曲时的纤芯折射率分布,虚线表示弯曲时的折射率分布。可看出当多芯光纤弯曲时,位于二、三象限的纤芯5的折射率变小,而位于一、四象限的纤芯2的折射率变大。

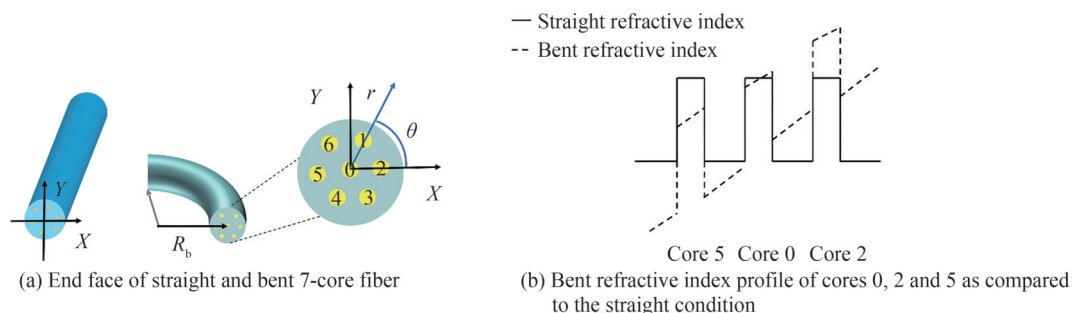


图1 弯曲对多芯光纤纤芯折射率的影响

Fig. 1 Influence of bending on refractive index of multi-core fiber

当纤芯的有效折射率发生变化时,纤芯群延时也会随之变化,将式(7)带入式(2)可得弯曲时的纤芯群延时为

$$\tau_{b,m} \approx \tau_m \left(1 + \frac{r_m}{R_b} \cos \theta_m \right) \quad (8)$$

因此由弯曲引起的纤芯群延时变化可表示为

$$\text{DGD}_{\text{cont}} = \tau_{b,m} - \tau_m = \frac{\tau_m r_m}{R_b} \cos \theta_m \quad (9)$$

由式(9)可看出,由弯曲引起的纤芯群延时变化与弯曲半径成反比,因此大弯曲半径有助于降低弯曲对多芯光纤纤芯群延时的影响。与式(7)类似,式(9)中当纤芯 m 和多芯光纤中心的连线与曲率面形成的夹角 $\theta = k\pi, k \in Z$ 时由弯曲引起的纤芯群延时变化最大,而当 $\theta = \pi/2 + k\pi, k \in Z$ 时由弯曲引起的纤芯群延时变化为零。

2 实验装置

基于空间干涉成像的多芯光纤芯间群延时差测量实验装置如图2所示,主要由可调谐激光器(Santec TSL-710, 1 480-1 640 nm)、单模光纤(Coming SMF-28e)、准直器(1 550 nm)、透镜、三维调节台、待测多芯光纤、物镜(60 \times)以及CCD(Hamamatsu C10633-23, 950~1 700 nm)组成。可调谐激光器输出的光,通过光纤连接器被耦合进单模光纤,经准直器准直后通过透镜聚焦再注入到待测纤芯中。其中,准直器和透镜的主要作用是减小入射光束的发散角,降低光能量损失,提升光束的传输和耦合效率。首先将多芯光纤两端擦净切平后分别固定在三维调节台1和2上,将多芯光纤的输出端接入光路I,组成一个多芯光纤纤芯选

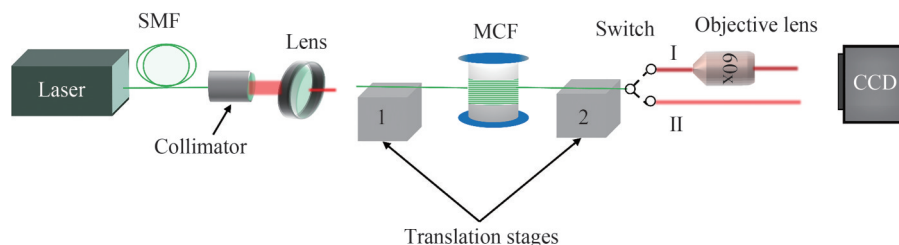


图2 基于空间干涉成像的多芯光纤芯间群延时差测量实验装置

Fig. 2 Experimental setup for the measure of the DGD in a multi-core fiber

择激发系统,当光注入多芯光纤后,调节三维调节台2,使得从CCD上可观察到清晰的光斑图。然后调节三维调节台1,使得通过CCD可观察到多芯光纤中待测纤芯的光斑图,而其余芯中几乎或完全无光场分布。当选择完待测纤芯后将光路转换到光路II,此时由于没有物镜的聚焦作用,待测纤芯的出射光处于发散的状态,且由于不同的纤芯具有不同的群延时,待测纤芯的出射光会在空间上相干叠加产生干涉。在多芯光纤出射端使用CCD记录不同波长下的空间干涉图,并从空间干涉图中提取空间干涉光谱,通过光谱分析可获得任意相邻两芯之间的群延时差。

3 七芯光纤芯间延时差测量结果

测量选取的七芯光纤为每个芯都只传输基模的沟槽辅助型弱耦合多芯光纤,沟槽辅助型多芯光纤通过在纤芯周围引入低折射率沟道,将光场最大限度地束缚在纤芯内部,从而降低相邻纤芯的芯间串扰。图3(a)为沟槽辅助型多芯光纤每个芯的三维折射率分布示意图。图3(b)是所测七芯光纤在显微镜下的端面图,七芯光纤外围的六个芯均匀地分布在以中间芯为中心的正六边形上,其任意相邻两个芯的芯间距为 $36.64\ \mu\text{m}$,为弱耦合多芯光纤(一般芯间距在 $35\sim 60\ \mu\text{m}$ 之间),每个芯的直径为 $5.55\ \mu\text{m}$,内沟槽直径为 $17.90\ \mu\text{m}$,外沟槽直径为 $25.72\ \mu\text{m}$ 。测量光纤长度为 $50\ \text{m}$,光纤弯曲半径为 $75\ \text{mm}$,波长范围为 $1\ 548\sim 1\ 552\ \text{nm}$ (带宽为 $4\ \text{nm}$),波长间隔为 $0.01\ \text{nm}$ 。因此,每测量一组数据可采集 401 张不同波长下的空间干涉图。

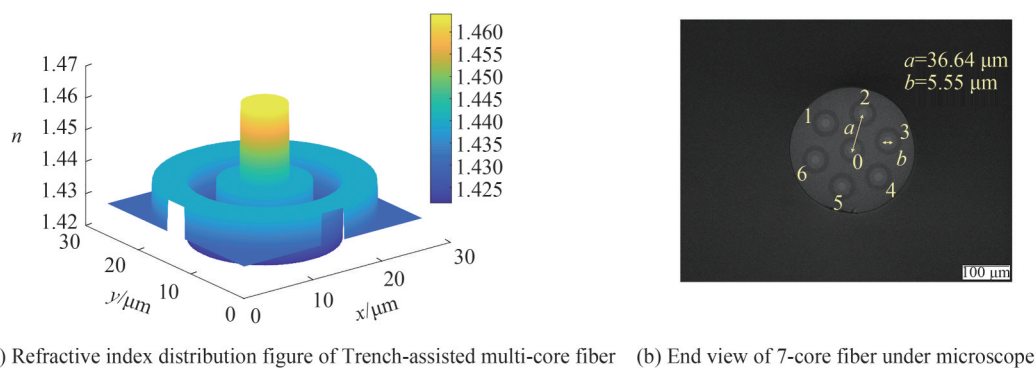


图3 沟槽辅助型多芯光纤
Fig. 3 Trench-assisted multi-core fiber

当光只耦合到两个相邻的芯中时,结构参数的差异会导致两个芯之间存在群延时差。因此,在待测光纤的出射端面会在空间上发生干涉。测量时,观察CCD并调节三维调节台来激发待测纤芯,而使其他芯保持未激发状态,图4(a)为在CCD上观察到的只激发中间芯和纤芯1时的情况。当完成待测纤芯的选择激发后,将光路转换到图2中的光路II,此时CCD拍摄到的图像为两芯间的空间干涉图,图4(b)为CCD采集到的 401 张中间芯和芯1的空间干涉图像,每张图片的分辨率为 256×320 ,深度为 $14\ \text{bit}$ 。

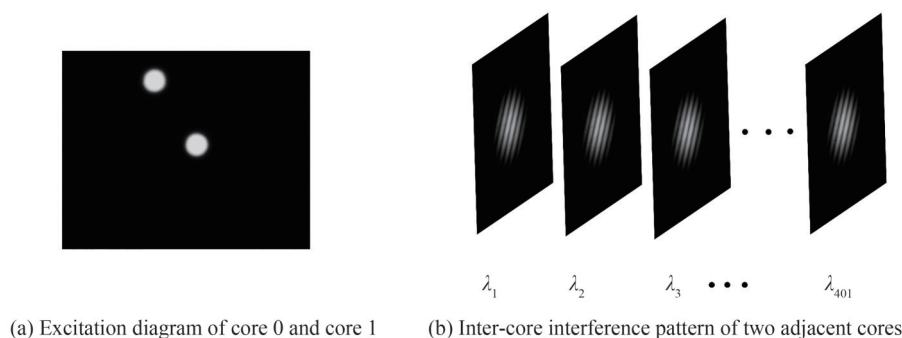


图4 纤芯0和纤芯1的激发图及空间干涉图
Fig. 4 Excitation diagram and spatial interference diagram of core 0 and core 1

图4(b)中,在每个波长下的空间干涉图中选取同一像素点 (x, y) ,该点的光强随波长变化而变化,形成的振荡曲线为这个点的空间干涉光谱,图5(a)为像素点(110, 185)处的空间干涉光谱。将所有像素点的空间干涉光谱在空间上组合在一起可得如图5(b)所示的三维空间干涉光谱。

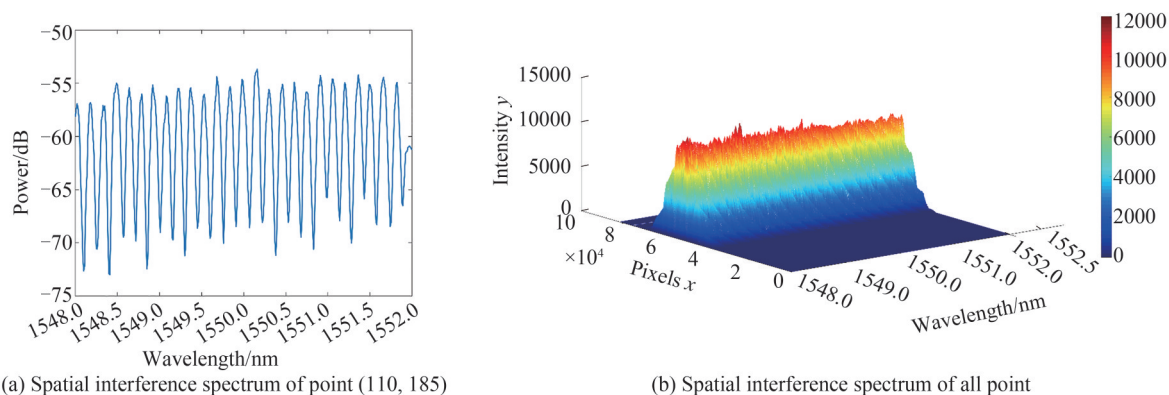


图5 纤芯0和纤芯1的空间干涉光谱

Fig. 5 Spatial interference spectra of core 0 and core 1

对图5(a)的空间干涉光谱做傅里叶变换的结果如图6(a)所示,可看出除中间芯与芯1的干涉尖峰外还有由噪声引起的尖峰,为了降低噪声的干扰,需要对图5(b)所示的所有点的空间干涉光谱同时做傅里叶变换,并将变换后的结果取模进行线性叠加,结果如图6(b)所示。从图6(b)中可看出由噪声产生的尖峰的能量远低于中间芯与芯1干涉产生的尖峰的能量,由干涉产生的尖峰的横坐标的值为 0.3994 ps/m ,为中间芯与芯1的芯间群延时差。

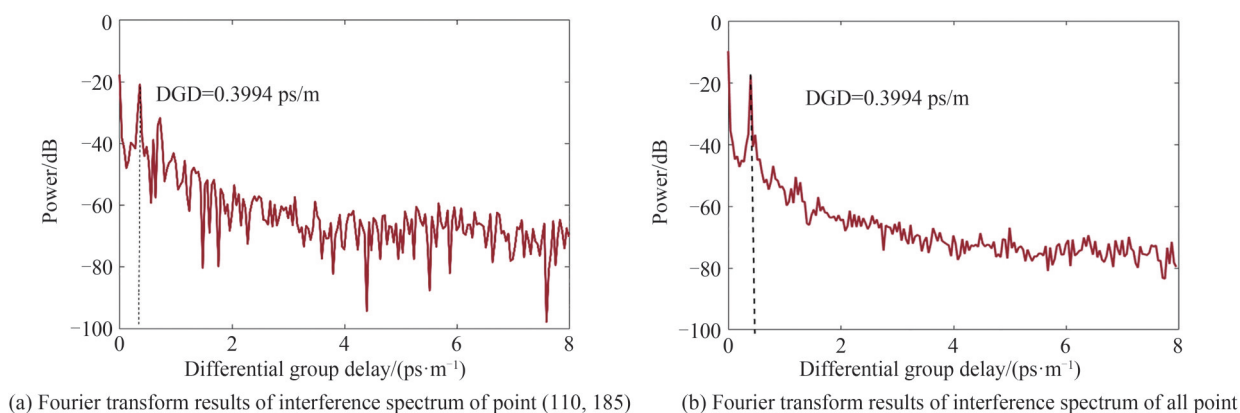


图6 纤芯0与纤芯1的空间干涉光谱分析结果

Fig. 6 Spatial interference spectrum analysis results of cores 0, 1

同理,当依次同时激发中间芯和一个外围芯时通过对空间干涉图像提取的所有像素点的空间干涉光谱做傅里叶变换并取模相加,可获得七芯光纤的中间芯与外围六个芯的芯间群延时差,图7(a)和(b)分别是中间芯与芯2以及中间芯和芯3的光谱分析结果。从图中可知中间芯与芯2的芯间群延时差为 0.5592 ps/m ,中间芯与芯3的芯间群延时差为 0.4394 ps/m 。

从图6和图7的测量结果来看,中间芯和不同外围芯的芯间群延时差都各不相同,说明在七芯光纤中任意两个相邻外围芯的群延时也会存在差异。图7中,将中间芯和芯2以及中间芯和芯3之间的芯间群延时差相减可获得芯2和芯3的芯间群延时差为 0.1198 ps/m 。

除了测量中间芯与外围芯的芯间群延时差,还可测量任意相邻两个外围芯的芯间群延时差。测量时同时激发芯2和芯3,而让其它芯保持未激发的状态。通过对两芯的空间干涉光谱进行光谱分析可获得两芯的芯间群延时差,分析结果如图8所示。由图8可知芯2和芯3的芯间群延时差为 0.1197 ps/m ,与 0.1198 ps/m 相近,误差为 1×10^{-4} 。

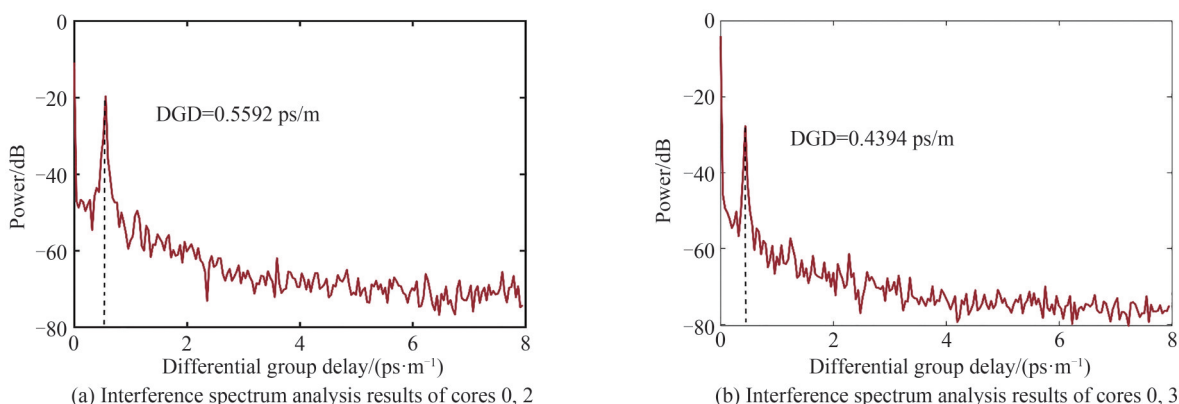


图7 中间芯0分别与外围芯2、芯3的空间干涉光谱分析结果
Fig. 7 Spatial interference spectrum analysis results of cores 0, 2 and cores 0, 3

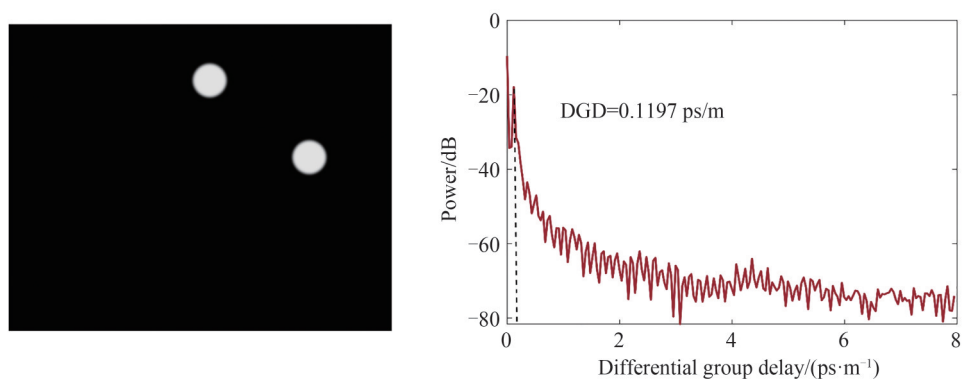


图8 同时激发纤芯2,3时的空间干涉光谱分析结果
Fig. 8 Spatial interference spectrum analysis results of core 2 and core 3

当同时激发三个纤芯时,相邻的芯会两两干涉,对干涉信息做傅里叶变换会出现三个干涉尖峰,图9是同时激发纤芯0、2和3时的测量结果。

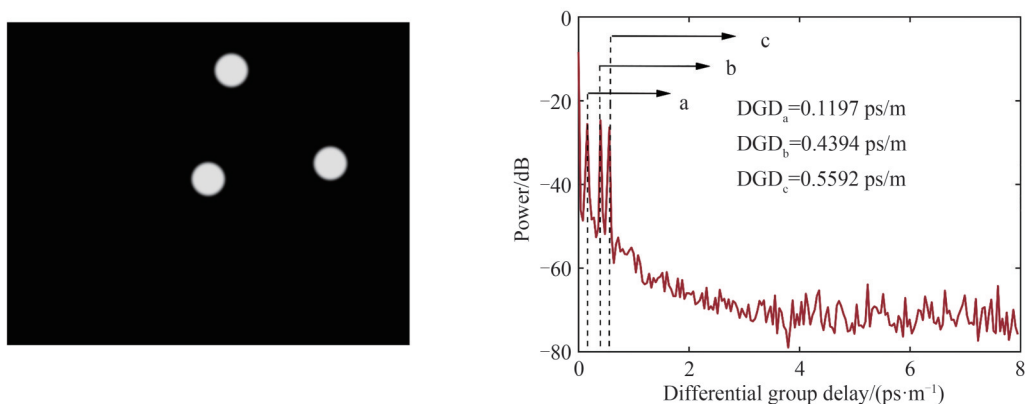


图9 同时激发纤芯0和纤芯2,3时的空间干涉光谱分析结果
Fig. 9 Spatial interference spectrum analysis results of cores 0, 2 and 3

图9中a、b、c三点处的群延时差分别为0.1197 ps/m、0.4394 ps/m以及0.5592 ps/m,将图9与图7和图8对比可看出三个群延时差的值分别一一对应。因此,图9中点a的值是芯2与芯3的芯间群延时差,点b和c的值分别是芯0和芯3、芯2的芯间群延时差。

同理,其它相邻芯之间也有相同的关系,表1展示了中间芯与其余6个外围芯、外围任意相邻两芯以及同时激发3个芯时的芯间群延时差测量结果。

表1 七芯光纤芯间群延时差测量结果
Table 1 Measurement results of the inter-core DGD of 7-core fiber

Cores		0-1	0-2	0-3	0-4	0-5	0-6	
Two cores	$-\Delta\tau/(\text{ps}\cdot\text{m}^{-1})$	0.399 4	0.559 2	0.439 4	0.159 8	0.439 4	0.679 0	
	Cores		1-2	2-3	3-4	4-5	5-6	6-1
	$\Delta\tau/(\text{ps}\cdot\text{m}^{-1})$	0.159 8	0.119 7	0.279 6	0.279 6	0.239 7	0.279 6	
Three cores	Cores		0-1-2	0-2-3	0-3-4	0-4-5	0-5-6	0-6-1
		$\Delta\tau_1/(\text{ps}\cdot\text{m}^{-1})$	0.159 8	0.119 7	0.159 8	0.159 8	0.239 6	0.279 6
		$\Delta\tau_2/(\text{ps}\cdot\text{m}^{-1})$	0.399 4	0.439 4	0.279 6	0.279 6	0.439 4	0.399 4
		$\Delta\tau_3/(\text{ps}\cdot\text{m}^{-1})$	0.559 2	0.559 2	0.439 4	0.439 4	0.679 0	0.679 0

任意两个相邻外围芯的芯间群延时差可通过将中间芯分别与外围两个相邻芯的芯间群延时差相减获得,也可直接测量外围相邻两芯的芯间群延时差。对比表1中的测量结果可发现任意两个相邻外围芯的芯间群延时差的直接测量结果与相减获得的结果相比,误差为 1×10^{-4} 。同时激发三个互相相邻纤芯时的测量结果与单独激发两个芯时的测量结果都一一对应,与理论一致且验证了测量结果的准确性。

4 七芯光纤芯间延时差弯曲依赖性测量结果

为了研究七芯光纤芯间延时差的弯曲依赖性,分别测量了长度为50 m,弯曲半径为5 mm、75 mm以及110 mm的七芯光纤,测量结果如表2所示。

表2 七芯光纤芯间群延时差的弯曲依赖性测量结果
Table 2 Measurement results of bending dependence of the inter-core DGD of 7-core fiber

Bending radius	Cores					
	0-1	0-2	0-3	0-4	0-5	0-6
5 mm	0.479 4	0.918 6	1.198 2	0.319 6	0.958 6	1.118 4
75 mm	0.399 4	0.559 2	0.439 4	0.159 8	0.439 4	0.679 0
110 mm	0.239 6	0.319 6	0.199 6	0.079 9	0.279 6	0.239 6

比较表2中三个不同弯曲半径的测量结果可发现,随着弯曲半径的增大,中间芯与外围芯的芯间群延时差不断减小,与理论分析一致。通过中间芯与外围芯的芯间群延时差的测量结果可计算出相邻外围芯之间的群延时差,随着弯曲半径的增大,外围芯的芯间群延时差也呈下降的趋势。

5 结论

本文提出了基于空间干涉成像的多芯光纤芯间群延时差测量方法,测量了七芯光纤芯间群延时差并研究了其芯间群延时差的弯曲依赖性。同时激发3个芯时的测量结果分别与只激发这3个芯中任意2个相邻纤芯时的测量结果一一对应,验证了测量结果的准确性,且测量误差仅为 1×10^{-4} ps/m,说明该方法不仅可测量两芯间的群延时差,还可同时测量多个芯之间的群延时差。当改变七芯光纤的弯曲半径时,芯间群延时差的测量结果会随着弯曲半径的增大而呈下降的趋势,与理论分析一致。提出的空间干涉成像法测量简单快速、精度高,可广泛应用于SDM系统和MWP信号处理等应用场景中多芯光纤的芯间延时差测量研究。

参考文献

- [1] OHASHI M, MATSUO S, HAYASHI T, et al. Optical fibers for space-division multiplexing [M]. Space-Division Multiplexing in Optical Communication Systems, Springer, 2022: 39-170.
- [2] TU Jiajing, QIAO Xihui, LONG Keping. Core arrangement method for few-mode multi-core fibres [J]. Acta Photonica Sinica, 2017, 46(1): 0106001.
涂佳静, 乔喜慧, 隆克平. 少模多芯光纤的纤芯排布方法 [J]. 光子学报, 2017, 46(1): 0106001.
- [3] WU Y, LUO H, CHENG M, et al. Capacity expansion of chaotic secure transmission system based on coherent optical detection and space division multiplexing over multi-core fiber [J]. Optics Letters, 2022, 47(3): 726-729.
- [4] NAKAJIMA K, MATSUI T, SAITO K, et al. Multi-core fiber technology: next generation optical communication strategy [J]. IEEE Communications Standards Magazine, 2017, 1(3): 38-45.

- [5] MATSUI T, SAGAE Y, SAKAMOTO T, et al. Design and applicability of multi-core fibers with standard cladding diameter [J]. *Journal of Lightwave Technology*, 2020, 38(21): 6065-6670.
- [6] GASULLA I, BARRERA D, HERVÁS J, et al. Spatial division multiplexed microwave signal processing by selective grating inscription in homogeneous multicore fibers [J]. *Scientific Reports*, 2017, 7(1): 41727.
- [7] UREÑA M, GARCÍA S, HERRANZ J I, et al. Experimental demonstration of dispersion-diversity multicore fiber optical beamforming [J]. *Optics Express*, 2022, 30(18): 32783-32790.
- [8] ZHAO Y, WANG C, ZHAO Z, et al. A microwave photonics true-time-delay system using carrier compensation technique based on wavelength division multiplexing[C]. *Proceedings of the Photonics*, 2022.
- [9] SHAHEEN S, GRIS-SÁNCHEZ I, GASULLA I. True-time delay line based on dispersion-flattened 19-core photonic crystal fiber [J]. *Journal of Lightwave Technology*, 2020, 38(22): 6237-6246.
- [10] MORANT M, TRINIDAD A, TANGDIONGGA E, et al. Multi-beamforming provided by dual-wavelength true time delay PIC and multicore fiber [J]. *Journal of Lightwave Technology*, 2020, 38(19): 5311-5317.
- [11] LUÍS R S, PUTTNAM B J, MENDINUETA J M D, et al. Impact of spatial channel skew on the performance of spatial-division multiplexed self-homodyne transmission systems [C]. *Proceedings of the 2015 International Conference on Photonics in Switching (PS)*, 2015.
- [12] PUTTNAM B J, LUÍS R S, RADEMACHER G, et al. Characteristics of homogeneous multi-core fibers for SDM transmission [J]. *APL Photonics*, 2019, 4(2): 022804.
- [13] LUIS R S, PUTTNAM B J, RADEMACHER G, et al. Compensation of inter-core skew in multi-core fibers with group velocity dispersion [J]. *Optics Express*, 2021, 29(18): 28104-28109.
- [14] SAKAMOTO T, MORI T, WADA M, et al. Experimental and numerical evaluation of inter-core differential mode delay characteristic of weakly-coupled multi-core fiber [J]. *Optics Express*, 2014, 22(26): 31966-31976.
- [15] LEE H J, MOON H S, KCHOI S, et al. Multi-core fiber interferometer using spatial light modulators for measurement of the inter-core group index differences [J]. *Optics Express*, 2015, 23(10): 12555-12561.
- [16] SASAKI Y, TAKENAGA K, AIKAWA K. Effect of bending on skew of multicore fibers and optical fiber ribbons[C]. *Proceedings of the 2020 Opto-Electronics and Communications Conference (OECC)*, 2020.
- [17] GARCÍA S, UREÑA M, GASULLA I. Bending and twisting effects on multicore fiber differential group delay [J]. *Optics Express*, 2019, 27(22): 31290-31298.
- [18] FU Xiaodong, PAN Hongfeng, FANG Honglian, et al. Comparative research of optimized coupled mode and coupled power theory in weakly coupled disturbed multi-core fibers [J]. *Acta Photonica Sinica*, 2022, 51(4): 0406003.
符小东, 潘洪峰, 房洪莲, 等. 优化耦合模和耦合功率理论在弱耦合扰动多芯光纤中的对比 [J]. *光子学报*, 2022, 51(4): 0406003.
- [19] GLOGE D. Weakly guiding fibers [J]. *Applied Optics*, 1971, 10(10): 2252-2258.
- [20] HU Lili, FENG Guoying, DONG Zheliang. Spatially and spectrally resolved fiber mode measurement method [J]. *Infrared and Laser Engineering*, 2015, 44(8): 2517-2522.
胡丽荔, 冯国英, 董哲良. 基于空间和频谱分辨的光纤模式测量方法 [J]. *红外与激光工程*, 2015, 44(8): 2517-2522.
- [21] GARCÍA S, UREÑA M, GASULLA I. Bending and twisting effects on multicore fiber differential group delay [J]. *Optics Express*, 2019, 27(22): 31290-31298.

Inter-core Differential Group Delay Measurement of Seven Core Fiber Based on Spatial Interference Imaging

SHEN Licui, HUANG Sujuan, CHEN Wei, YAN Cheng, ZHAO Xinpeng

(Key Laboratory of Specialty Fiber Optics Access Networks, School of Communication and Information Engineering, Shanghai University, Shanghai 200444, China)

Abstract: Using different cores of a Multi-Core Fiber (MCF) as independent parallel spatial paths to transmit different information simultaneously offers cost, space and energy savings. The inter-core Differential Group Delay (DGD) is a key parameter of the multi-core fibers, and its accurate measurement is of great importance. In the multi-core fibers, errors in the preparation process or bending of the fiber caused by external forces can result in inter-core differential group delay in various cores. When light is transmitted in a multi-core fiber, the outgoing light from different cores will interfere with coherent superposition in space due to different group delays. According to this character, this paper proposes a

spatial interferometric imaging-based method for measuring the inter-core differential group delay of multi-core fibers, and building an experimental measurement device. At the input of the multi-core fiber, the laser is shifted and injected by adjusting the three-dimensional adjustment table to excite different cores, and the output light of the excited cores will interfere in space. The computer controls the CCD to scan the wavelength of the input light in one dimension and records the spatial interferogram at different wavelengths in real time. The interferometric information of all pixels in the interferogram is used to construct a three-dimensional spatial interferometric spectrum, and the inter-core differential group delay of the multi-core fiber can be obtained by spectral analysis of the interferometric spectrum. The inter-core differential group delay of the weakly linked trench assisted seven core fiber is measured in this paper. We measured the inter-core differential group delay between the central and six outer cores respectively. When two cores are excited at the same time, a peak will appear at the delay difference between the two cores through the Fourier transform of the interference information. Subtracting the inter-core differential group delay between the central core and two adjacent outer cores yields the inter-core differential group delay between the two outer cores, which is only 10^{-4} dissimilar from the actually measured inter-core differential group delay of two adjacent outer cores. When three spikes are excited simultaneously, two adjacent spikes will interfere with each other. By Fourier transforming the interference information obtained by CCD containing the differential group delay, a plot of differential group delay versus interference intensity containing three spikes can be constructed. The values of the horizontal coordinates of the three spikes in the plot are the differential group delay between the three cores, and they correspond to the measurement results when only any two of the three cores are excited, respectively. Simultaneously, the bending dependence of the inter-core DGD of the multi-core fiber is measured and researched. The inter-core differential group delay was measured for three bending radii of 5 mm, 75 mm, and 110 mm. The results reveal that the inter-core DGD decreases as the bending radius increases, which is consistent with the theory. This method's measurement instrument is simple, and the measuring precision can reach 10^{-4} . It can measure the delay difference not only between two cores, but also between any nearby cores at the same time. In addition, the outgoing light from the end face of the multi-core fiber to be measured is focused through the objective lens and connected to the CCD and adjust the three-dimensional adjustment table, the excitation state of the cores in the multi-core fiber and the degree of coupling of optical energy can be observed on the CCD, which makes the selection and excitation of the cores to be measured easier. The spatial interference imaging approach suggested in this study has the characteristics of simple, fast, high accuracy. It can be widely used to measure inter-core DGD of the multi-core fiber in SDM systems, MWP signal processing and other application circumstances.

Key words: Spatial interference imaging; Spectrum analysis; Weakly-coupled seven core fiber; Inter-core difference group delay; Bending dependence

OCIS Codes: 060.2300; 060.2350; 060.2605; 070.4790